Water Research X 28 (2025) 100314

Contents lists available at ScienceDirect

Water Research X

journal homepage: www.sciencedirect.com/journal/water-research-x

Microbial mechanisms underlying the reduction of N_2O emissions from submerged plant covered system

Yongxia Huang [a,b,c,1], Min Deng [b,1], Shuni Zhou [b,c], Yunpeng Xue [b,c], Senbati Yeerken [b,c], Yuren Wang [b,c], Lu Li [a,b], Kang Song [a,b,c,d,*]

[a] National-Regional Joint Engineering Research Center for Soil Pollution Control and Remediation in South China, Guangdong Key Laboratory of Integrated Agro-environmental Pollution Control and Management, Institute of Eco-environmental and Soil Sciences, Guangdong Academy of Sciences, Guangzhou 510650, PR China
[b] State Key Laboratory of Freshwater Ecology and Biotechnology, Key Laboratory of Lake and Watershed Science for Water Security, Institute of Hydrobiology, Chinese Academy of Sciences, Wuhan 430072, PR China
[c] University of Chinese Academy of Sciences, Beijing 100049, PR China
[d] Southern Marine Science and Engineering Guangdong Laboratory (Guangzhou), Guangzhou 511458, PR China

ARTICLE INFO

Keywords:
Plant restoration
Leaf-attached biofilm
Counter-diffusion
Nitrification rate
N_2O reduction rate
Greenhouse gas

ABSTRACT

Submerged plant (SP) restoration is a crucial strategy for restoring aquatic ecosystem. However, the effect of SP on nitrous oxide (N_2O) emissions remains controversial, and the impact of SP-attached biofilms on N_2O emissions is often overlooked. In this study, SP and non-submerged plant (NSP) systems were set up and operated continuously for 189 days, revealing that SP reduced N_2O flux by 42.4 %. By comparing the N_2O net emission rates from water, sediment, and biofilms, we identified biofilms as the primary medium responsible for the reduction in N_2O emissions in both SP and NSP systems. Further analysis of N_2O metabolic rates from nitrification, denitrification, and abiotic processes under light and dark conditions confirmed that counter-diffusion of dissolved oxygen and nutrients in SP biofilms plays a key role in reducing denitrification-driven N_2O emissions. Additionally, SP-attached biofilms increased *nosZII*-type denitrifiers (e.g., *Bacillus*) and reduced N_2O production potential ((*nirS*+*nirK*)/(*nosZI*+*nosZII*)). Notably, the establishment of a SP restoration project in a typical eutrophic freshwater lake demonstrated that SP could reduce N_2O fluxes by 61.5 %. This study provides significant insights for strategies aimed at mitigating N_2O emissions.

1. Introduction

Nitrous oxide (N_2O) is a potent greenhouse gas, with a warming potential 298 times that of carbon dioxide (IPCC, 2013). It also acts as an ozone-depleting substance (Yu et al., 2013). Between 1750 and 2018, N_2O levels have increased by 20 %, showing a consistent growth rate of 2 % per decade (Thompson et al., 2019). Freshwater ecosystems account for 10 %–17 % of anthropogenic N_2O emissions (Qin et al., 2019). The eutrophication of freshwater ecosystems and subsequent decline in submerged plant (SP) biomass are widespread ecological issues (Xiao et al., 2019). However, the impact of SP on N_2O fluxes remains uncertain.

Recently, limited field observations have reported on the effects of SP restoration, plant types, plant abundance, and SP-dominated zones on N_2O flux (Davidson et al., 2015; Li et al., 2024; Ni et al., 2022). However, there is still no clear consensus on the impact of SP on N_2O emissions. SP-dominant zones in lakes were found to be associated with lower nutrient levels and lower N_2O concentrations compared to algae, free-floating plants, and open water, indicating a potential reduction in N_2O emissions (Aben et al., 2022; Ni et al., 2022; Wang et al., 2009a). But more plants were found to lead to increased N_2O emissions due to ecosystem instability and the decay of SP (Davidson et al., 2015). Other environmental factors, e.g., nutrients, usually became the dominant environmental factor affecting N_2O emission in lakes due to spatial heterogeneity (Xiao et al., 2019). Therefore, exploring N_2O emissions in both SP and non-plant (NSP) areas under similar nutrient conditions is crucial. Additionally, the photosynthesis of SP contributes to enhanced diel variation in N_2O flux (Ni et al., 2022), but the specific effects of light and dark conditions on N_2O metabolic processes need further explore. The epiphytic biofilm attached to SP stems and leaves plays a crucial role

* Corresponding author at: Donghu South road No 7, Wuhan city, Hubei province, PR China.
E-mail address: sk@ihb.ac.cn (K. Song).
[1] Y.H. and M.D. contributed equally to this work.

https://doi.org/10.1016/j.wroa.2025.100314
Received 29 November 2024; Received in revised form 3 February 2025; Accepted 5 February 2025
Available online 7 February 2025

in nitrogen cycling and N_2O production. However, the key N_2O metabolic microbial processes in the epiphytic biofilm and their differences compared to NSP attached biofilms are still not well understood.

N_2O emissions are primarily driven by nitrification (as a byproduct) and incomplete denitrification ($NO_3^- \rightarrow NO_2^- \rightarrow NO \rightarrow N_2O$), as extensively documented in epiphytic biofilms (Ni et al., 2022; Wang et al., 2023a). Moreover, the last step of denitrification ($N_2O \rightarrow N_2$) serves as primary microbial mechanism for N_2O reduction (Wang et al., 2009a). Unlike biofilms attached to NSP carriers (e.g., bedrock, gravel, and sand), which exhibit co-diffusion of nutrients and oxygen, SP attached biofilms exhibit counter-diffusion during photosynthesis (Fig. S1). This counter-diffusion biofilm resembles membrane-aerated biofilms, suggesting a potential mitigation of N_2O emissions (Kinh et al., 2017). SP provides a specific niche for nitrifiers and may stimulate denitrification through the retention of labile organic detritus or the release of organic matter from leaf cells (Coci et al., 2008; Jiang et al., 2024b; Wang et al., 2009a). However, the disparities in the layered nitrifying and denitrifying community structure between SP and NSP biofilms, as well as their impacts on N_2O emissions, remain unclear.

Here, we examine how SP affects nitrification and denitrification

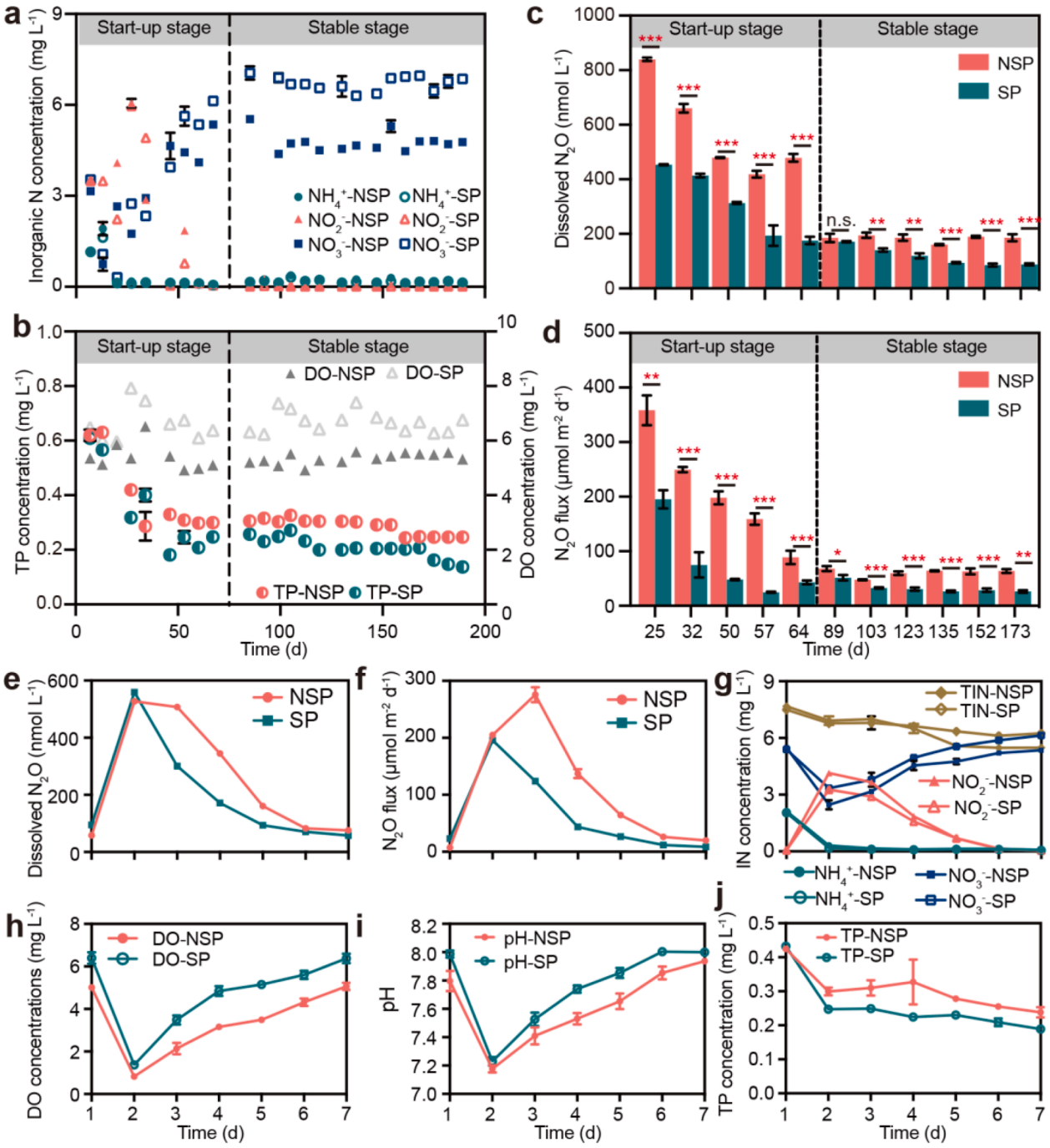

Fig. 1. Environmental factors and N_2O emission characteristics in mesocosm systems. a-b Long-term NH_4^+-N, NO_2^--N, NO_3^--N, TP, and dissolved oxygen (DO) concentrations variation in mesocosm systems. c-d Long-term dissolved N_2O concentrations and N_2O fluxes variation in mesocosm systems. Error bars represent standard deviations of triplicate tests. e-j The variation of dissolved N_2O concentration, N_2O fluxes, inorganic nitrogen concentration, dissolved oxygen (DO) concentration, pH and total phosphorus (TP) concentration during a single cycle in NSP and SP mesocosm systems during a single cycle. *, **, and *** means significance levels at $p < 0.05$, $p < 0.01$, and $p < 0.001$, respectively.

rates and associated N_2O emission in mesocosm systems. The impacts of layered biofilm structure and light-dark conditions on N_2O emission in water, sediment, and attached biofilms were also investigated. Furthermore, the abundance of nitrifying and denitrifying functional genes and the microbial community structure in surface, interior, and total biofilms were analyzed to elucidate the underlying microbial mechanism of N_2O emissions. These findings help fill the current knowledge gap regarding N_2O emissions in SP and NSP areas of shallow lakes, with implications for strategies to mitigate greenhouse gas emissions.

2. Results

2.1. Long-term N_2O emission characteristics in NSP and SP systems

The environmental factors and N_2O emissions in mesocosm systems over long term (189 days) are shown in Fig. 1. During the stable stage, concentrations of dissolved oxygen (DO) and nitrate nitrogen (NO_3^--N) were significantly higher in the SP system than the NSP system (Table S1). Conversely, total phosphorus (TP) and nitrite nitrogen (NO_2^--N) concentrations in SP system were significantly lower than NSP system ($p < 0.05$). The average dissolved N_2O concentration (183.4 ± 4.0 nmol L^{-1}) and N_2O flux (61.2 ± 1.8 μmol m^{-2} D^{-1}) in NSP system were 1.7- and 1.8-fold higher than SP system (105.6 ± 2.6 nmol $L^{-1}$and 33.7 ± 1.6 μmol m^{-2} D^{-1}, respectively) ($p < 0.05$) (Fig. 1c-d). Hence, SP system significantly mitigated N_2O emissions over the long term compared to the NSP system.

2.2. N_2O emission characteristics in NSP and SP systems during a single cycle

During the 17th cycle, the total inorganic nitrogen (TIN) concentrations gradually decreased from 7.6 ± 0.11 mg L^{-1} to 5.5 ± 0.1 mg L^{-1} and 6.2 ± 0.1 mg L^{-1} in NSP and SP systems, respectively (Fig. 2g). The SP system exhibited a significantly higher DO concentration than NSP system (Table S2) ($p < 0.01$). Both DO concentration and pH experienced a significant decrease on day 2, followed by a gradual increase to their initial levels by day 7. The dissolved N_2O concentrations significantly increased from 76.5 ± 20.5 nmol L^{-1} to 543.1 ± 19.1 nmol L^{-1} on day 2, before declining to 66.8 ± 9.8 nmol L^{-1} by day 7 (Fig. 1e). Notably, from day 3 to day 7, both dissolved N_2O concentrations and N_2O fluxes in NSP system were significantly higher than SP system ($p < 0.01$). Therefore, SP system effectively reduced N_2O emissions during a single cycle.

2.3. Influence of dark and light on the potential N_2O metabolic rate

In NSP system, there was no significant difference in N_2O fluxes between light(47.7 ± 0.7 μmol m^{-2} D^{-1}) and dark (46.0 ± 0.7 μmol m^{-2} D^{-1}) ($p > 0.05$) (Fig. 2c). However, in SP system, the N_2O fluxes were significantly higher under light (32.7 ± 1.1 μmol m^{-2} D^{-1}) than dark (10.8 ± 3.8 μmol $m^{-2}d^{-1}$) ($p < 0.05$). Notably, N_2O fluxes in both systems were consistent with total N_2O net emission rates of nitrification, denitrification, and abiotic processes (Fig. 2d). Additionally, in NSP system, there was no significant difference observed in potential total denitrifying N_2O production rate (N_2O_{DNP}), potential total denitrifying N_2O reducing rate (N_2O_{DNR}) and nitrification rate between dark and light ($p > 0.05$) (Fig. 2f-h). However, in SP system, both N_2O_{DNP} and N_2O_{DNR}, significantly decreased, while nitrification rate significantly increased under light compared to dark ($p < 0.01$) (Fig. 2f-h). The potential denitrifying N_2O net emission rates (N_2O_{DNE}) of NSP biofilm was significantly higher than that of SP biofilm under both dark and light (Fig. 2e). Furthermore, the N_2O_{DNE} of water and sediment under dark and light conditions exhibited no significant difference between NSP and SP systems (Fig. 2e). Hence, the disparity in N_2O fluxes can be attributed to the contribution of the attached biofilm.

To investigate the impact of complete leaf-attached biofilm structure on N_2O emission, the leaf-attached biofilm was separated to broke layered biofilm structure (Fig. S1). Broking the layered biofilm structure significantly reduced the N_2O_{DNP}, N_2O_{DNR}, and N_2O_{DNE} of leaf-attached biofilm ($p < 0.05$) (Fig. 2k-m).

2.4. N_2O production and reduction related functional genes in leaf-attached biofilms

In SP biofilms, the abundance of *AOB-amoA, napA*, and *nosZII* genes was significantly higher ($p < 0.001$), while *Comammox-amoA, narG, nirS, nirK*, and *nosZI* genes were significantly lower than NSP biofilms ($p < 0.05$) (Fig. 3a). Moreover, the N_2O production potential, indicated by (*nirS*+*nirK*)/(*nosZI*+*nosZII*) ratio, were higher in NSP biofilm than SP biofilm (Fig. 3b). The leaf-attached biofilm presents a stratified structure, comprising both interior and surface layers (Fig. 3c). The interior biofilm harbored significantly higher abundance of AOB-*amoA, napA, nirS, nirK, nosZI*, and *nosZII* than surface biofilm in both NSP and SP systems (Fig. 3d-k). In NSP system, *narG* abundance was significantly higher in interior biofilm ($p < 0.001$), but no significant difference was found in SP system ($p > 0.05$). Notably, N_2O production potential ((*nirS*+*nirK*)/(*nosZI*+*nosZII*)) was higher in interior biofilm of NSP system, whereas SP system showed the opposite trend (Fig. 3l).

2.5. Microbial community of total leaf-attached biofilms, interior biofilms, and surface biofilms

PCoA1 and PCoA2 explained 52.99 % and 21.65 % of microbial community variation, respectively, indicated a distinct clustering of microbial communities between NSP and SP attached biofilms (Fig. 4a). Notably, microbial communities in interior biofilms of NSP system were similar to those in surface biofilms of SP system. The phyla *Firmicutes* was significantly less abundant in NSP biofilms than in SP biofilms ($p < 0.05$) (Fig. 4b). Additionally, in NSP system, *Nitrospirae* and *Planctomycetes* were significantly more abundant in interior biofilms than in surface biofilms ($p < 0.05$), while *Firmicutes* showed opposite trend ($p < 0.05$). Conversely, in SP system, *Nitrospirae* was more abundant in surface biofilms than in interior biofilms ($p < 0.05$). In NSP biofilms, the abundance of *Nitrosomonadaceae* (AOB) and *Nitrospirae* was higher than in SP biofilms (Fig. 4c-d). These results indicated that significant differences in microbial communities between NSP and SP biofilms, warranting further exploration at the genus level.

Among denitrifiers at genus level, *Rhodobacter* and *Gemmobacter* were significantly more abundant in NSP biofilms than in SP biofilm, while *Bacillus* showed opposite trend (Fig. 4g) (Lei et al., 2021). In NSP system, *Rhodobacter, Thauera*, and *Gemmobacter* were less abundant in surface biofilms than interior biofilms, whereas *Bacillus* and *Pseudomonas* exhibited opposite trend (Fig. 4g) (Huang et al., 2023; Wang et al., 2023c). Conversely, in SP system, *Bacillus* and *Pseudomonas* were less abundant in surface biofilms than in interior biofilms, while *Gemmobacter* showed opposite trend. In NSP attached biofilms, *Nitrosomonas* was the core nitrifier but showed no significant association with core denitrifiers such as *Rhodobacter, Pseudomonas*, and *Thauera* (Fig. 4h). Conversely, in SP attached biofilms, *Nitrosomonas* was positive correlated with the denitrifier *Gemmobacter*. Additionally, *Pseudomonas* and *Thauera* were identified as core denitrifiers in SP biofilm (Fig. 4i). These findings highlight significant differences in the distribution and associations of denitrifiers between NSP and SP layered biofilms.

2.6. N_2O emission from SP and NSP area in freshwater lake

To validate the findings from our indoor mesocosm experiments, we implemented a large-scale field trial in Donghu Lake. In this engineering experiment, 20,000 m^2 of submerged plants were cultivated to evaluate their impact on N_2O emissions under natural conditions. The results showed that dissolved N_2O concentrations in SP area (11.5 ± 1.6 nmol L^{-}

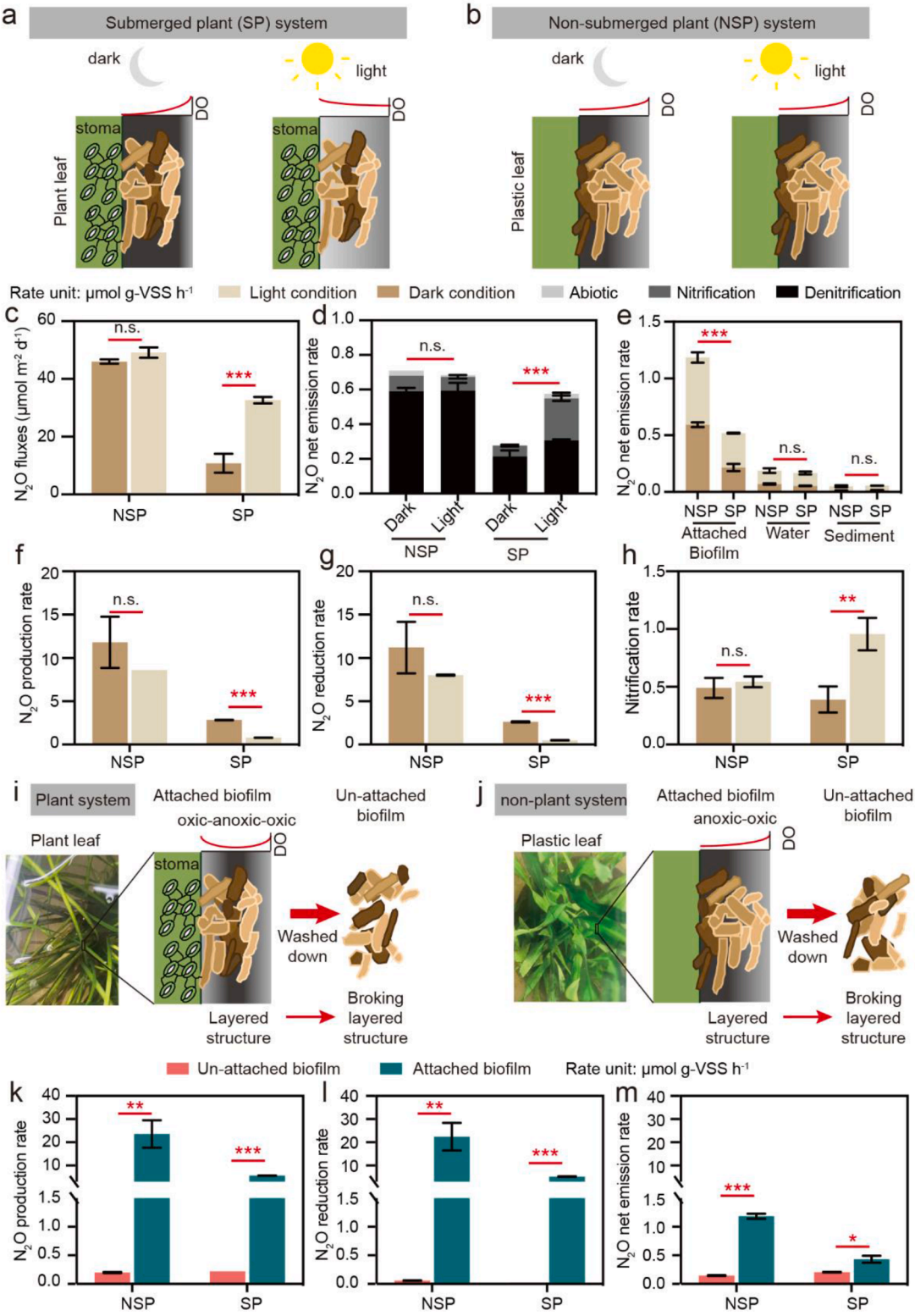

Fig. 2. The N_2O flux and N_2O metabolic rates in submerged plant (SP) system and non-submerged plant (NSP) system under dark and light conditions. a-b Schematic diagram showing the difference of dissolved oxygen (DO) concentration variation in the attached biofilm in SP system and NSP system. c The N_2O fluxes in NSP and SP systems under dark and light conditions. d The N_2O net emission rates of attached biofilm in NSP and SP systems during denitrification, nitrification, and abiotic processes. e The N_2O net emission rates of attached biofilm, water, and sediment in NSP and SP systems. f-g The N_2O production rate and N_2O consumption rate during denitrification in NSP and SP systems under dark and light conditions. h The nitrification rates in NSP and SP systems under dark and light conditions. i-j Schematic diagram showing the difference of attached biofilm and washed down un-attached biofilm in SP system and NSP system. k-m The N_2O production rate, N_2O consumption rate, and N_2O net emission rate of un-attached biofilm and attached biofilm in NSP and SP systems. *, ** and *** represent significance levels at $p < 0.05$, $p < 0.01$, and $p < 0.001$, respectively. n.s. represents no significance ($p > 0.05$).

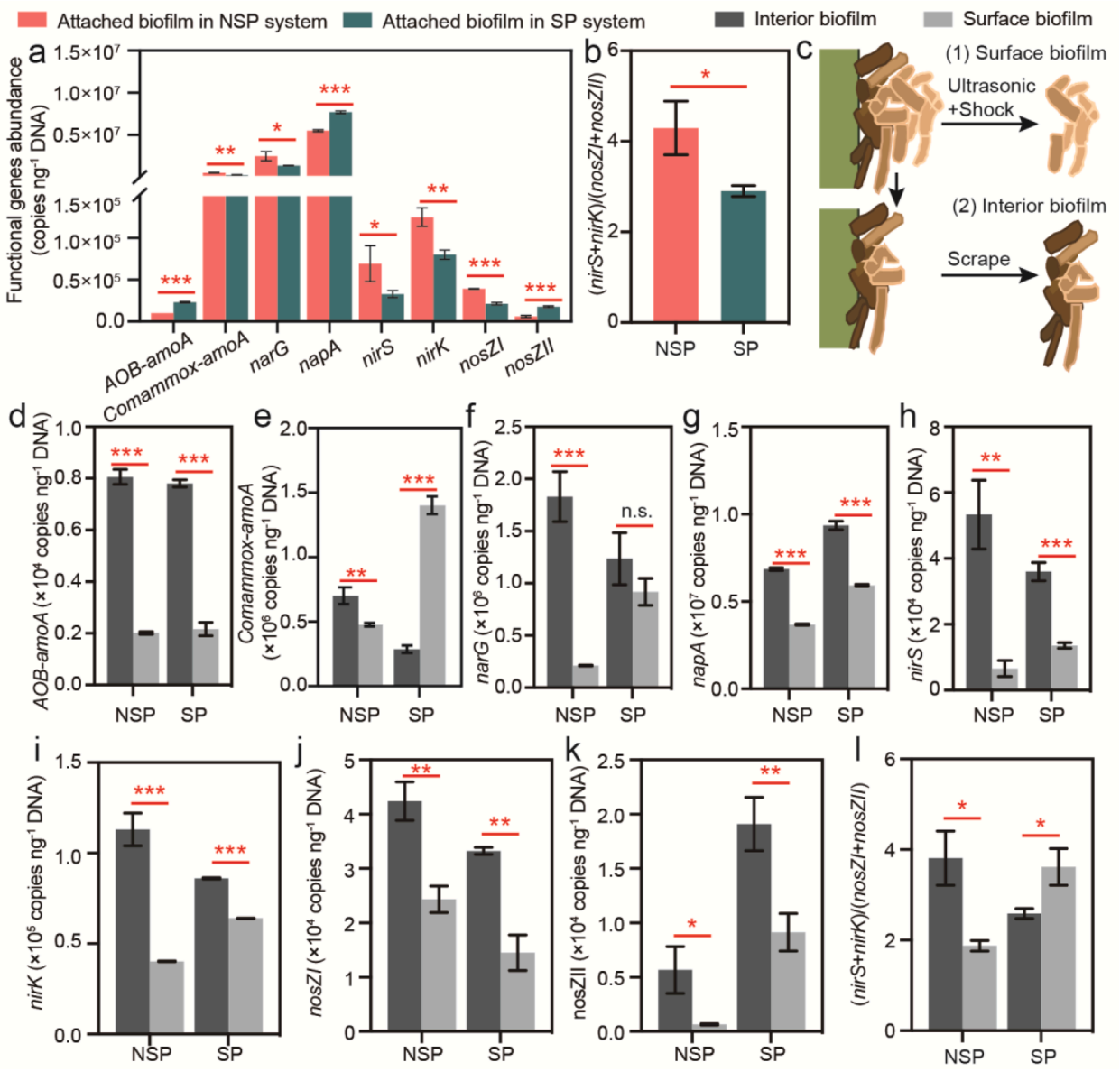

Fig. 3. The N_2O metabolic related functional genes abundance of attached biofilms, interior biofilms, and surface biofilms in non-submerged plant (NSP) and submerged plant (SP) systems. a The functional genes abundance of attached biofilms in NSP and SP systems. b The (*nirS*+*nirK*)/(*nosZI*+*nosZII*) ratio of attached biofilms in NSP and SP systems. c Schematic diagram showing the difference of interior biofilm and surface biofilm. d-l The abundance of AOB-*amoA*, Comammox-*amoA, narG, napA, nirS, nirK, nosZI, nosZII* genes, and (*nirS*+*nirK*)/(*nosZI*+*nosZII*) ratio of interior biofilm and surface biofilm in NSP and SP systems. *, **, and *** represent significance levels at $p < 0.05$, $p < 0.01$, and $p < 0.001$, respectively.

^{1}) were significantly lower than those in NSP area (13.9 ± 1.7 nmol L^{-1}) ($p < 0.05$) (Fig. 5e). N_2O saturability was 136.4 ± 18.5 % and 171.3 ± 19.7 % for SP and NSP areas, respectively (Fig. 5f). Field-measured N_2O fluxes in NSP area (11.7 ± 8.4 μmol m^{-2} D^{-1}) were on average 2.6 times of those in SP area (4.5 ± 2.9 μmol m^{-2} D^{-1}) (Fig. 5g). In SP area, the pH and DO concentration were significantly higher than NSP area. Notably, there was no significant difference in NH_4^+-N, NO_2^--N, NO_3^--N, and total nitrogen (TN) from water column, between NSP and SP areas (Table 1). The large-scale field trial also confirmed that SP can effectively reduce N_2O emissions under natural conditions.

3. Discussion

3.1. The key microbial process for N_2O emission

The lower N_2O emission in SP system compared to NSP system is attributed to leaf-attached biofilm, not water or sediment (Fig. 2e). Previous studies indicated that SP restoration does not enhance nitrogen removal rates or denitrifiers abundances in sediment (Liu et al., 2018; Yao et al., 2018). Denitrification accounted for 84.74 ± 2.08 % and 64.37 ± 12.90 % of N_2O production for NSP and SP biofilms, respectively (Fig. 2d). The higher denitrification-driven N_2O production in NSP biofilms led to higher N_2O emissions than SP biofilms (Fig. 2d). This is consistent with higher N_2O production potential ((*nirS*+*nirK*)/(*nosZI*+*nosZII*)) in NSP biofilms than SP biofilms ($p < 0.05$) (Fig. 3b).

Microbial respiration reduces DO concentration, while SP photosynthesis increases it (Yan et al., 2018) (Fig. 1h). The different DO micro-profiles in SP and NSP attached biofilms altered the abundance of denitrifying functional genes (Dong et al., 2014) (Fig. 3). For N_2O production, *narG* encodes obligate anaerobic nitrate reductase, while *napA* encodes aerobic nitrate reductase (Wang et al., 2023c). Additionally,

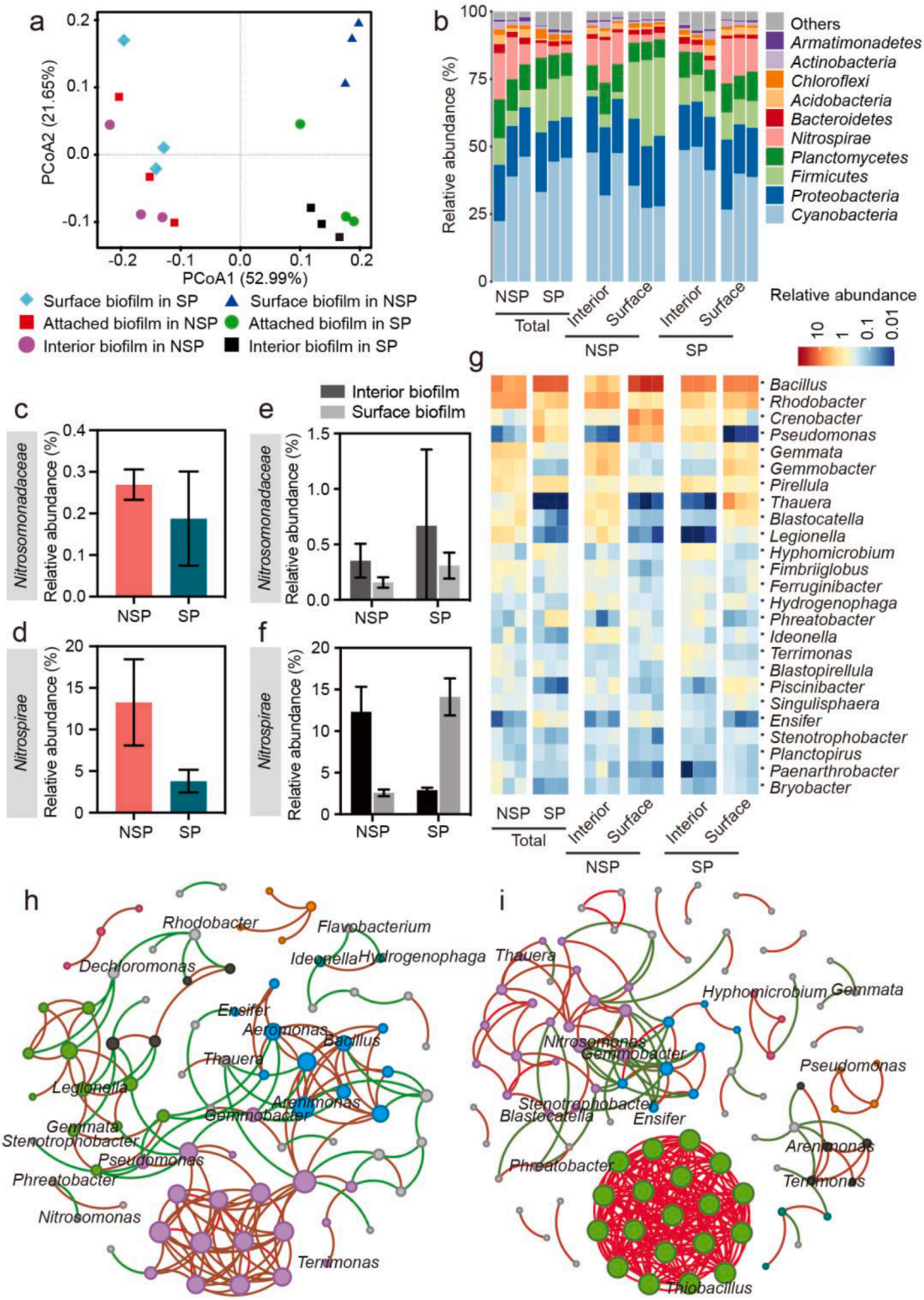

Fig. 4. Microbial community structure and interaction of total biofilm, interior biofilm, and surface biofilm in non-submerged plant (NSP) and submerged plant (SP) systems. a PCoA analysis of microbial community composition in attached biofilms, interior biofilms, and surface biofilms in NSP and SP systems. b Microbial community structure of top 10 phyla (average abundance in all samples) of interior biofilms and surface biofilms in NSP and SP systems. c-d The relative abundance of order *Nitrosomonadaceae* (AOB) and phylum *Nitrospirae* (comammox/nitrite-oxidizing bacteria) in attached biofilms in NSP and SP systems. e-f The relative abundance of order *Nitrosomonadaceae* (AOB) and phylum *Nitrospirae* (including comammox) in interior biofilm and surface biofilm in NSP and SP systems. g Heatmap of top 25 genera (average abundance in all samples) of attached biofilms, interior biofilms and surface biofilms in NSP and SP systems. h-i Co-occurrence networks in NSP and SP systems. Attached biofilm, interior biofilm, and surface biofilm were used for co-occurrence networks analysis. A connection stands for a strong (Spearman's $\rho \geq 0.6$) and significant (False discovery rate-adjusted p-value < 0.001) correlation. The nodes were colored by modularity class, and the size of each node was corresponding to the number of connections (i.e., degree). The red lines indicate positive correlations, while green lines express negative correlations. (For interpretation of the references to colour in this figure legend, the reader is referred to the web version of this article.)

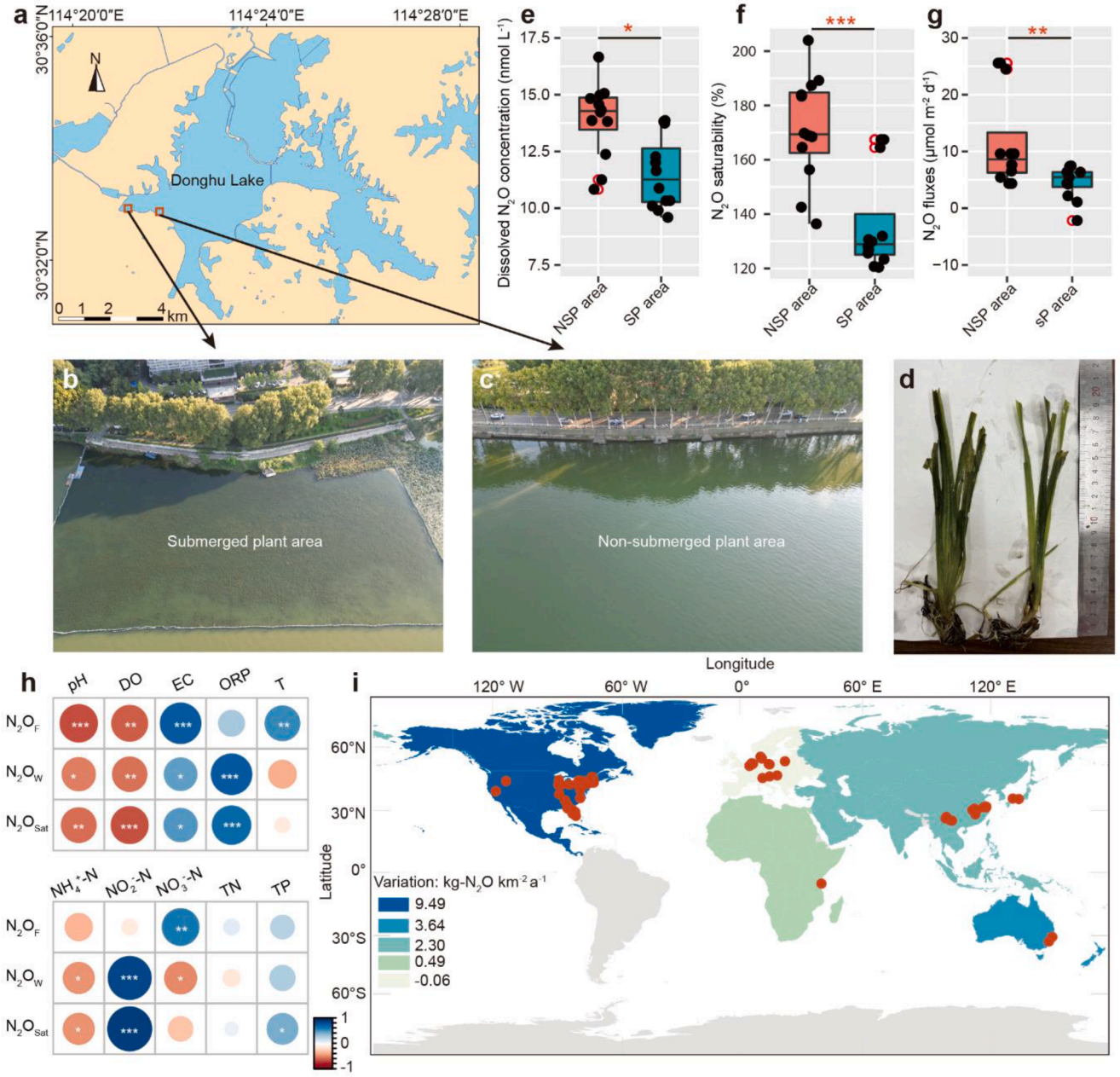

Fig. 5. Sampling sites and N_2O emission in Donghu Lake of Wuhan city. a Location map of submerged plant (SP) area and non-plant (NSP) areas. b-c Field status of SP area and NSP area, respectively. d The photo of dominant submerged plant *Vallisneria natans*. e-g The dissolved N_2O concentration, N_2O saturability, and N_2O fluxes in NSP and SP areas. h Spearman correlation between N_2O flux (N_2O_f), dissolved N_2O concentration (N_2O_w), N_2O saturability (N_2O_{sat}) and environmental factors. i Average N_2O emission variation estimated from global intercontinental lake submerged plant coverage.

nirS gene encode obligate anaerobic nitrite reductase, while *nirK* gene encodes facultative anaerobic nitrite reductase (Song et al., 2022). Hence, the lower abundance of *narG, nirS*, and *nirK* in SP biofilm than NSP biofilm was attributed to higher DO concentration (Table S2). This explained the higher N_2O_{DNP} in NSP biofilm than SP biofilm (Fig. 2f). Furthermore, *nosZII*-type denitrifiers demonstrated a high O_2 inhibition constant and recover faster after O_2 exposure than *nosZI*-type denitrifiers (Zhou et al., 2020). Moreover, *nosZII*-type denitrifiers have a high affinity for N_2O, and have advantage in reducing low concentration of N_2O to N_2 in SP biofilm (Suenaga et al., 2019). Despite nitrification and microbial respiration lowering pH (Yan et al., 2018) (Fig. 1i), the pH remains within suitable range for microbial denitrification (Pan et al., 2012). Therefore, DO emerges as the key environmental factor affecting denitrification and resulting in low N_2O emission in the SP system.

The photosynthetic oxygen released by SP under light condition enhanced nitrification (Fig. 2h) and nitrification-driven N_2O emissions (Fig. 2d) in SP biofilm. Previous studies showed no significant difference in N_2O fluxes between day and night in NSP areas ($p > 0.05$), while SP areas had significantly higher daytime N_2O fluxes ($p < 0.01$) (Ni et al., 2022). Photosynthetic oxygen was benefit for traditional nitrifier (AOB) in SP biofilm ($p < 0.001$) (Fig. 3a) (Yan et al., 2018). Conversely, the abundance of comammox, a low DO-adapted and low N_2O-producing nitrifier (Kits et al., 2019; Roots et al., 2019), was lower in SP biofilm than NSP biofilm. Consequently, under light condition, the nitrification-driven N_2O emission rate was comparable to denitrification-driven N_2O emission rate in SP biofilm (Fig. 2d). Overall, although photosynthetic oxygen increased nitrification-driven N_2O release in SP system under light condition, it inhibited

Table 1
The environmental factors in non-submerged plant (NSP) and submerged plant (SP) areas of Donghu Lake, Wuhan.

Parameters	NSP area	SP area
pH[a]	8.6 ± 0.3	10.2 ± 0.4***
DO (mg L^{-1})[a]	8.4 ± 0.9	13.3 ± 0.3***
EC (μs cm^{-1})[a]	400.3 ± 42.8	314.0 ± 19.4***
ORP (mV)[a]	53.8 ± 12.4	25.7 ± 23.2***
T (°C)[a]	28.5 ± 3.3	27.88±3.5
TAN (mg L^{-1})[a]	0.1 ± 0.0	0.1 ± 0.0
NO_2^--N (mg L^{-1})[a]	0.02±0.00	0.02±0.00
NO_3^--N (mg L^{-1})[a]	0.1 ± 0.1	0.1 ± 0.1
TN (mg L^{-1})[a]	0.5 ± 0.2	0.4 ± 0.5
TP (mg L^{-1})[a]	0.07±0.01	0.05±0.01**

[a] Independent sample Mann-Whitney U test was used for significance analysis. ** and *** mean significance levels at $p < 0.01$ and $p < 0.001$, respectively.

denitrification-driven N_2O release, leading to overall lower N_2O emission in SP system than NSP system.

3.2. Different layered microbial structure of attached biofilm

Complete biofilm structures were indispensable for N_2O metabolism in both NSP and SP biofilm (Fig. 2). Micro-probe measurements indicated that as the distance from the plant surface decreases, DO concentration gradually increases (Dong et al., 2014). This counter-diffusion of DO and nitrogen nutrients in SP biofilm led to lower N_2O emissions than co-diffusion in NSP biofilm during simultaneous nitrification and denitrification (Kinh et al., 2017). Interestingly, despite DO concentration gradient difference between NSP and SP biofilms (Fig. 1h), interior biofilm in both systems supported the growth of nitrifiers and denitrifiers (Fig. 3d-k) (Zhang et al., 2022). While surface biofilms, which are prone to detachment, hindered nitrifiers and denitrifiers (Fig. 3d-k). Importantly, interior and surface biofilm served as denitrifying N_2O producing hotspots in NSP and SP biofilms, respectively (Fig. 3l). Consequently, high DO concentration in surrounding water environment inhibited surface biofilm in SP system, resulting in low denitrification-driven N_2O emissions (Fig. 2e). Unlike nitrifying and denitrifying functional genes, the microbial community structures of interior and surface biofilms differed significantly between NSP and SP biofilms (Fig. 4). Denitrifiers such as *Bacillus* (aerobic), *Pseudomonas* (aerobic), and *Gemmobacter* (anoxic) exhibited varied abundance distributions in interior and surface biofilms of both NSP and SP biofilms, primarily due to differences in oxygen tolerance (Liu et al., 2020a; Wang et al., 2019a, 2023c). The distinct functional and microbial community differences between NSP and SP layered biofilms highlight the critical influence of SP in creating oxygen gradients that mitigate denitrification-driven N_2O emissions, emphasizing the ecological importance of SP recovery for reducing greenhouse gas production in aquatic environments.

3.3. Submerged plant reduced N_2O emission from freshwater ecosystems

The SP system reduced N_2O fluxes by 42.4 % compared to NSP system (Fig. 1c). Similarly, SP restoration decreased 61.5 % of N_2O emissions from a typical freshwater lake (Fig. 5g). Previous studies reported lower dissolved N_2O concentrations (4.6~46.3 nmol L^{-1}) and N_2O fluxes (−1.7~29.5 μmol m^{-2} D^{-1}) in SP system than NSP system (11.5~98.8 nmol L^{-1} and 2.4~54.9 μmol m^{-2} D^{-1}, respectively) (Table S8) (Ni et al., 2022; Wang et al., 2009b). Typically, N_2O fluxes are positively correlated with TIN (Fig. 5h) (Song et al., 2022). However, there were no significant differences in NH_4^+-N, NO_2^--N, and NO_3^--N concentrations between NSP and SP areas (Table 1) ($p > 0.05$). Therefore, the increased pH and DO concentration in SP area should affect microbial process, reducing N_2O flux (Table 1; Fig. 5g) (Ni et al., 2022). The key microbial processes and environmental factors affecting N_2O emission in NSP and SP systems were further investigated.

Eutrophication often triggers algae blooms and decline in SP coverage (Yan et al., 2018). From the 1960s to 1990s, Donghu lake transitioned from moderate to severe eutrophication (Xie and Xie, 2002), causing SP coverage to drop from over 60 % to <1 % (Wang et al., 2019b). Our study suggests that restoring SP coverage to 60 % could reduce N_2O emissions by about 2.2 t a^{-1} in Donghu Lake. Additionally, decreased SP biomass generally increases N_2O emissions in lakes worldwide, particularly in North America (9.49 kg N_2O km^{-2} a^{-1}) (Table S12). Therefore, restoring SP helps mitigate global warming by reducing N_2O emissions.

4. Conclusion

Human-induced eutrophication of aquatic environments globally has led to decline in submerged plant coverage in lakes. This disruption of nitrogen cycling has resulted in increased N_2O emissions. The difference in N_2O levels between NSP and SP systems primarily stems from leaf-attached biofilm rather than water and sediment. The intact structure of biofilm and its counter-current diffusion of DO and nutrients play a crucial role in mitigating N_2O emissions. Despite plant photosynthesis increasing N_2O production through nitrification in leaf-attached biofilm, the significant reduction in denitrification-associated N_2O production ultimately decreases N_2O emissions in SP areas. Through the establishment of a submerged plant restoration project in Donghu Lake, we found that submerged plant restoration could reduce N_2O fluxes by 61.5 %. These findings shed light on the mechanisms underlying global SP degradation, altering nitrification, denitrification, and associated N_2O fluxes. Finally, restoring SP is an effective management measure to mitigate N_2O emissions in eutrophic lakes.

5. Materials and methods

5.1. Setup and operation of NSP and SP mesocosm ecosystems

Two 1000-L cylindrical tanks were established as indoor mesocosm ecosystems to simulate the effect of submerged plants on N_2O emissions in a lake environment. These tanks (800 L), with a working volume of 400 L and a water depth of 40 cm, were labeled as NSP and SP systems. In the SP system, four 10-L cylindrical tanks were planted with *Vallisneria natans*. To avoid biofilm structure differences caused by variations in carrier shape and surface area, artificial plastic plants made of polyvinyl chloride (PVC), a durable and non-biodegradable material, resembling *Vallisneria natans* were planted in four 10-L cylindrical tanks within the NSP system. Sediment from Donghu lake was used to fill these tanks, ensuring homogeneity. Both *Vallisneria natans* and plastic plants, purchased from the local market, were planted at a density of 50 plants m^{-2} to achieve a similar surface area for biofilm attachment. To maintain optimal conditions, the water temperature in each system was regulated at 25 °C utilizing five 500 W heating rods. Furthermore, a lighting schedule of 12 h of light (at 4000 lux, provided by three 14 W seedling lamps) alternating with 12 h of darkness was implemented in both systems.

Following a 7-day pre-cultivation period, the mesocosm systems ran continuously for 189 days. To maintain initial concentrations of 40 mg L^{-1} chemical oxygen demand (COD), 2 mg L^{-1} NH_4^+-N, 6 mg L^{-1} NO_3^--N, and 0.4 mg L^{-1} total TP for both NSP and SP systems, a stock solution was added weekly based on the measured nutrient concentrations after the 7-day cultivation cycles. All other experimental procedures and daily maintenance activities remained consistent across both systems. Weekly, the overlying water was collected for water quality analysis. Dissolved N_2O concentrations and N_2O fluxes in both NSP and SP systems were periodically detected during the start-up and stable stages. To investigate the impact of photosynthesis, measurements of dissolved N_2O concentrations and fluxes were conducted under both light and dark conditions (day 89 and 103). Additionally, at the end of the stable

stage, dissolved N_2O concentrations, N_2O fluxes, and water quality were assessed daily over a 7-day period.

5.2. N_2O emission characteristics from SP and NSP areas in freshwater lake

A field experiment was further conducted in an urban freshwater lake (Donghu Lake, China). In April, *Vallisneria natans* (50 plants m^{-2}) was planted in a lakeshore area (SP area) covering approximately 20,000 m^2 (Fig. 5a). Donghu lake spans 31.8 km^2 and is a shallow, eutrophic freshwater lake located in a subtropical monsoon climate region (Qiu et al., 2001). N_2O emission characteristics were studied in the SP area (E114°21′6″, N30°32′53″) and the adjacent NSP area (E114°21′47″, N30°32′ 49″) from July to October, coinciding with the peak biomass of the submerged plants. N_2O fluxes were evaluated using the floating chamber method, while dissolved N_2O concentrations in the water were determined using the headspace equilibrium method (Song et al., 2022). Further details on sample collection, measurement, and calculation procedures can be found in the Supplementary Information. Monthly samples of overlying water (20 cm depth) were collected for water quality analysis. A meta-analysis was performed to evaluate changes in the biomass of global SP and their potential impact on N_2O emissions. Refer to the Supporting Information for further details.

5.3. Inorganic nitrogen and N_2O metabolic rate during nitrification, denitrification, and abiotic processes under light and darkness conditions

The potential nitrification rate and potential nitrifying N_2O net emission rate (N_2O_{NE}) was determined using the potassium chlorate inhibition method (Zhang et al., 2023) and the 0.01 % (*v/v*) acetylene inhibition method (Jiang et al., 2023), respectively. Additionally, the potential denitrification rate, potential total denitrifying N_2O production rate (N_2O_{DNP}), potential denitrifying N_2O net emission rates (N_2O_{DNE}), and potential total denitrifying N_2O reducing rate (N_2O_{DNR}) were determined using the 10 % (v/v) acetylene inhibition method (Jiang et al., 2024a). The potential abiotic N_2O net emission rate ($N_2O_{abiotic}$) was determined using the saturated $ZnCl_2$ inhibition method (Fig. S3) (Wang et al., 2023b). Specifically, 5 g of leaf with attached biofilm (wet weight) were placed in a 120 mL serum bottle containing synthetic water for the measurement of potential nitrification and denitrification rate, N_2O_{DNP}, N_2O_{DNE}, N_2O_{DNR}, and $N_2O_{abiotic}$. Additionally, 2 g of fresh leaf with attached biofilm (wet weight) was placed into individual 20 mL serum vials, with each vial receiving 0.5 mL culture solution (Table S6) to submerge the leaf for N_2O_{NE} measurement. For more details, refer to the Supporting Information.

5.4. Comparison of denitrifying N_2O net emission rates of attached biofilm, water, and sediment in NSP and SP systems

During the stable stage, leaf-attached biofilm, water, and sediment samples were collected from NSP and SP systems on day 150 for N_2O_{DNE} analysis. The leaf-attached biofilm was collected following the procedure described above. For water samples, 1 L of water was filtered through a 0.22 μm membrane, and the particles on the filter were washed into a 120 mL serum bottle using 10 mL synthetically wastewater (Table S5). Regarding sediment samples, after removing stones and plant debris, the sediment was washed twice with sterile ultrapure water to eliminate existing nutrients. Then, 5 g of sediment were added to a 120 mL serum bottle for N_2O_{DNE} analysis, following the same procedure mentioned above.

5.5. Comparison the N_2O metabolic rate of leaf-attached biofilm and unattached biofilm

To explore the impact of the complete structure of leaf-attached biofilm on N_2O metabolism, we compared the N_2O metabolic rate during denitrification between the leaf-attached biofilm and the unattached biofilm. Initially, the unattached biofilm was obtained by subjecting it to 10 min of ultrasound, followed by 30 min of shock treatment, and another 10 min of ultrasound. Subsequently, the strongly attached biofilm was gently scraped off using a sterile surgical blade. Finally, the N_2O_{DNP}, N_2O_{DNE}, and N_2O_{DNR} were evaluated following the same procedure as described above.

5.6. Water quality analysis

Water temperature, DO concentration, pH, electrical conductivity (EC), and oxidation–reduction potential (ORP) were measured 20 cm below the surface water using a HQ3d multi-parameter analyzer (HACH, USA). Concentrations of NH_4^+-N, nitrite nitrogen (NO_2^--N), and NO_3^--N, TN, and TP were determined in triplicate following standard method (APHA, 2012). Total inorganic nitrogen (TIN) represents the sum of NH_4^+-N, NO_2^--N, and NO_3^--N.

5.7. Microbial community function and composition in surface biofilm, interior biofilm, and total biofilm

For microbial DNA extraction, approximately 20 g of NSP and SP leaves with biofilms were submerged in 200 mL of 0.5 M phosphate buffer (pH=7.4). After 10 min of ultrasound treatment, surface biofilm samples were collected. Subsequently, interior biofilms were obtained by subjecting the samples to 30 min of agitation (225 r min^{-1}), followed by 10 min of ultrasound treatment (Liu et al., 2020b). The strongly attached biofilm was then gently scraped off using a sterile surgical blade. Additionally, total biofilms, comprising both surface and interior biofilms, were obtained from new samples. The biofilm suspensions were filtered through a sterile 50-μm sieve mesh to remove leaves. After centrifugation at 5000 rpm for 15 mins and removal of the supernatant, the collected biofilms were stored at −20 °C for DNA extraction.

DNA extraction was performed using the DNeasy PowerSoil kit (Qiagen, Hilden, Germany). Real-time quantitative PCR (qPCR) was used to quantify nitrification and denitrification-related functional genes (Huang et al., 2024). The functional genes assessed included AOB-*amoA*, Comammox-*amoA, narG, napA, nirS, nirK, nosZI*, and *nosZII* (Table S10). Additionally, PacBio sequencing was performed at Novogene, China (Song et al., 2020). Further information on PacBio sequencing, library construction, and taxonomy annotation can be found in the Supporting Information. All PacBio sequencing data and sample information are available at National Center for Biotechnology Information (NCBI) Sequence Read Archive database at https://www.ncbi.nlm.nih.gov/bioproject/PRJNA1097465.

5.8. Statistical analysis

Statistical analysis was conducted using SPSS 26.0 (SPSS Inc., Chicago, USA). The normality of the water physicochemical parameters, dissolved N_2O concentration, N_2O flux, N_2O saturability, and functional gene abundance was assessed using the Shapiro-Wilk test. For normally distributed data, independent-samples *t*-test was employed, while the Kruskal-Wallis sum test was utilized for non-normally distributed data. Spearman correlation analysis was used to evaluate the relationships between N_2O emission characteristics and environmental factors. Co-occurrence network analysis was performed on NSP and SP biofilm samples to identify core nitrifiers and denitrifiers and explore their interactions (Song et al., 2022). Principal Coordinates Analysis (PCoA), Spearman correlation analysis, and co-occurrence network analysis were conducted using R software (version 4.0.4).

CRediT authorship contribution statement

Yongxia Huang: Writing – review & editing, Writing – original draft, Data curation, Conceptualization. **Min Deng:** Writing – review &

editing, Validation, Supervision, Formal analysis, Data curation, Conceptualization. **Shuni Zhou:** Data curation. **Yunpeng Xue:** Visualization. **Senbati Yeerken:** Methodology. **Yuren Wang:** Software. **Lu Li:** Conceptualization. **Kang Song:** Supervision, Funding acquisition.

Declaration of competing interest

The authors declare that they have no known competing financial interests or personal relationships that could have appeared to influence the work reported in this paper.

Acknowledgments

This work was supported by the National Natural Science Foundation of China (Grant No 42222709; 42307505; 42107277), GDAS' Project of Science and Technology Development (2023GDASZH-2023010103; 2022GDASZH-2022010104-2; 2020GDASYL-20200101002), National key research and development program of China (Grant no 2023YFC3205801), Hubei Provincial Natural Science Foundation of China (2022CFA109), Project of southern marine science and engineering Guangdong laboratory (Guangzhou) (BYQ20231202), Guangdong Major Project of Basic and Applied Basic Research (2023B0303000006).

Supplementary materials

Supplementary material associated with this article can be found, in the online version, at doi:10.1016/j.wroa.2025.100314.

Data availability

Data will be made available on request.

References

Aben, R.C.H., Velthuis, M., Kazanjian, G., Frenken, T., Peeters, E., Van de Waal, D.B., Hilt, S., de Senerpont Domis, L.N., Lamers, L.P.M., Kosten, S., 2022. Temperature response of aquatic greenhouse gas emissions differs between dominant plant types. Water Res 226, 119251.

APHA, 2012. Standard Methods For the Examination of Water and Wastewater, 22 th ed. American Public Health Association, American Water Works Association, Water Environment Federation, Washshington, D.C.

Coci, M., Bodelier, P.L., Laanbroek, H.J., 2008. Epiphyton as a niche for ammonia-oxidizing bacteria: detailed comparison with benthic and pelagic compartments in shallow freshwater lakes. Appl. Environ. Microbiol. 74, 1963–1971.

Davidson, T.A., Audet, J., Svenning, J.C., Lauridsen, T.L., Sondergaard, M., Landkildehus, F., Larsen, S.E., Jeppesen, E., 2015. Eutrophication effects on greenhouse gas fluxes from shallow-lake mesocosms override those of climate warming. Glob. Chang. Biol. 21, 4449–4463.

Dong, B., Han, R., Wang, G., Cao, X., 2014. O_2, pH, and redox potential microprofiles around Potamogeton malaianus measured using microsensors. PLoS ONE 9, e101825.

Huang, S., Zhang, B., Zhao, Z., Yang, C., Zhang, B., Cui, F., Lens, P.N.L., Shi, W., 2023. Metagenomic analysis reveals the responses of microbial communities and nitrogen metabolic pathways to polystyrene micro(nano)plastics in activated sludge systems. Water Res 241, 12016.

Huang, Y., Li, L., Li, R., Li, B., Wang, Q., Song, k., 2024. Nitrogen cycling and resource recovery from aquaculture wastewater treatment systems: a review. Environ. Chem. Lett. 1–16.

IPCC, 2013. Climate Change 2013: the physical science basis. Contribution of Working Group I to the Fifth Assessment Report of the Intergovernmental Panel On Climate Change. Cambridge University Press, USA.

Jiang, L., Liu, S., Wang, S., Sun, L., Zhu, G., 2024a. Effect of tillage state of paddy soils with heavy metal pollution on the nosZ gene of N_2O reductase. J. Environ. Sci. 137, 469–477.

Jiang, L., Yu, J., Wang, S., Wang, X., Schwark, L., Zhu, G., 2023. Complete ammonia oxidization in agricultural soils: high ammonia fertilizer loss but low N_2O production. Glob. Chang. Biol. 29, 1984–1997.

Jiang, X., Wang, M., Yang, S., He, D., Fang, F., Yang, L., 2024b. The response of structure and nitrogen removal function of the biofilm on submerged macrophytes to high ammonium in constructed wetlands. J. Environ. Sci. 142, 129–141.

Kinh, C.T., Suenaga, T., Hori, T., Riya, S., Hosomi, M., Smets, B.F., Terada, A., 2017. Counter-diffusion biofilms have lower N_2O emissions than co-diffusion biofilms during simultaneous nitrification and denitrification: insights from depth-profile analysis. Water Res 124, 363–371.

Kits, K.D., Jung, M.-Y., Vierheilig, J., Pjevac, P., Sedlacek, C.J., Liu, S., Herbold, C., Stein, L.Y., Richter, A., Wissel, H., Brüggemann, N., Wagner, M., Daims, H., 2019. Low yield and abiotic origin of N_2O formed by the complete nitrifier *Nitrospira* inopinata. Nat. Commun. 10, 1836.

Lei, L., Gu, J., Wang, X., Song, Z., Yu, J., Wang, J., Dai, X., Zhao, W., 2021. Effects of phosphogypsum and medical stone on nitrogen transformation, nitrogen functional genes, and bacterial community during aerobic composting. Sci. Total Environ. 753, 141746.

Li, Q., Yu, H., Yuan, P., Liu, R., Jing, Z., Wei, Y., Tu, S., Gao, H., Song, Y., 2024. Mitigated N_2O emissions from submerged-plant-covered aquatic ecosystems on the Changjiang River Delta. Sci. Total Environ. 928, 172592.

Liu, T., He, X., Jia, G., Xu, J., Quan, X., You, S., 2020a. Simultaneous nitrification and denitrification process using novel surface-modified suspended carriers for the treatment of real domestic wastewater. Chemosphere 247, 125831.

Liu, W., Jiang, X., Zhang, Q., Li, F., Liu, G., 2018. Has submerged vegetation loss altered sediment denitrification, N_2O production, and denitrifying microbial communities in subtropical lakes? Global Biogeochem. Cy. 32, 1195–1207.

Liu, Y., Gong, L., Mu, X., Zhang, Z., Zhou, T., Zhang, S., 2020b. Characterization and co-occurrence of microbial community in epiphytic biofilms and surface sediments of wetlands with submersed macrophytes. Sci. Total Environ. 715, 136950.

Ni, M., Liang, X., Hou, L., Li, W., He, C., 2022. Submerged macrophytes regulate diurnal nitrous oxide emissions from a shallow eutrophic lake: a case study of Lake Wuliangsuhai in the temperate arid region of China. Sci. Total Environ. 811, 152451.

Pan, Y., Ye, L., Ni, B.J., Yuan, Z., 2012. Effect of pH on N_2O reduction and accumulation during denitrification by methanol utilizing denitrifiers. Water Res 46, 4832–4840.

Qin, X., Li, Y., Goldberg, S., Wan, Y., Fan, M., Liao, Y., Wang, B., Gao, Q., Li, Y., 2019. Assessment of indirect N_2O emission factors from agricultural river networks based on long-term study at high temporal resolution. Environ. Sci. Technol. 53, 10781–10791.

Qiu, D., Wu, Z., Liu, B., Deng, J., Fu, G., He, F., 2001. The restoration of aquatic macrophytes for improving water quality in a hypertrophic shallow lake in Hubei Province. China. Ecol. Eng. 18, 147–156.

Roots, P., Wang, Y., Rosenthal, A.F., Griffin, J.S., Sabba, F., Petrovich, M., Yang, F., Kozak, J.A., Zhang, H., Wells, G.F., 2019. Comammox *Nitrospira* are the dominant ammonia oxidizers in a mainstream low dissolved oxygen nitrification reactor. Water Res 157, 396–405.

Song, J.M., Guan, Z., Hu, J., Guo, C., Yang, Z., Wang, S., Liu, D., Wang, B., Lu, S., Zhou, R., Xie, W.Z., Cheng, Y., Zhang, Y., Liu, K., Yang, Q.Y., Chen, L.L., Guo, L., 2020. Eight high-quality genomes reveal pan-genome architecture and ecotype differentiation of Brassica napus. Nat. Plants 6, 34–45.

Song, K., Senbati, Y., Li, L., Zhao, X., Xue, Y., Deng, M., 2022. Distinctive microbial processes and controlling factors related to indirect N_2O emission from agricultural and urban rivers in Taihu watershed. Environ. Sci. Technol. 56, 4642–4654.

Suenaga, T., Hori, T., Riya, S., Hosomi, M., Smets, B.F., Terada, A., 2019. Enrichment, isolation, and characterization of high-affinity N_2O-reducing bacteria in a gas-permeable membrane reactor. Environ. Sci. Technol. 53, 12101–12112.

Thompson, R.L., Lassaletta, L., Patra, P.K., Wilson, C., Wells, K.C., Gressent, A., Koffi, E. N., Chipperfield, M.P., Winiwarter, W., Davidson, E.A., Tian, H., Canadell, J.G., 2019. Acceleration of global N_2O emissions seen from two decades of atmospheric inversion. Nat. Clim. Change 9, 993–998.

Wang, D., Gan, X., Wang, Z., Jiang, S., Zheng, X., Zhao, M., Zhang, Y., Fan, C., Wu, S., Du, L., 2023a. Research status on remediation of eutrophic water by submerged macrophytes: a review. Process Saf. Environ. 169, 671–684.

Wang, S., Liu, C., Yeager, K.M., Wan, G., Li, J., Tao, F., Lu, Y., Liu, F., Fan, C., 2009a. The spatial distribution and emission of nitrous oxide (N_2O) in a large eutrophic lake in eastern China: anthropogenic effects. Sci. Total Environ. 407, 3330–3337.

Wang, S., Liu, C., Yeager, K.M., Wan, G., Li, J., Tao, F., Lǔ, Y., Liu, F., Fan, C., 2009b. The spatial distribution and emission of nitrous oxide (N_2O) in a large eutrophic lake in eastern China: anthropogenic effects. Sci. Total Environ. 407, 3330–3337.

Wang, S., Zhao, J., Ding, X., Zhao, R., Huang, T., Lan, L., Naim Bin Nasry, A.A., Liu, S., 2019a. Effect of starvation time on NO and N_2O production during heterotrophic denitrification with nitrite and glucose shock loading. Process Biochem 86, 108–116.

Wang, T., Wang, Q., Xia, S., Yan, C., Pei, G., 2019b. Response of benthic algae to environmental conditions in an urban lake recovered from eutrophication. China. J. Oceanol. Limnol. 38, 93–101.

Wang, X., Wang, S., Yang, Y., Tian, H., Jetten, M.S.M., Song, C., Zhu, G., 2023b. Hot moment of N_2O emissions in seasonally frozen peatlands. ISME J 17, 792–802.

Wang, Y., Deng, M., Li, B., Li, L., Oon, Y.S., Zhao, X., Song, K., 2023c. High nitrous oxide (N_2O) greenhouse gas reduction potential of Pseudomonas sp. YR02 under aerobic condition. Bioresour. Technol. 378, 128994.

Xiao, Q., Xu, X., Zhang, M., Duan, H., Hu, Z., Wang, W., Xiao, W., Lee, X., 2019. Coregulation of nitrous oxide emissions by nitrogen and temperature in China's third largest freshwater lake (Lake Taihu). Limnol. Oceanogr. 64, 1070–1086.

Xie, L., Xie, P., 2002. Long-term (1956–1999) dynamics of phosphorus in a shallow, subtropical Chinese lake with the possible effects of cyanobacterial blooms. Water Res 36, 343–349.

Yan, L., Zhang, S., Lin, D., Guo, C., Yan, L., Wang, S., He, Z., 2018. Nitrogen loading affects microbes, nitrifiers and denitrifiers attached to submerged macrophyte in constructed wetlands. Sci. Total Environ. 622-623, 121–126.

Yao, L., Chen, C., Liu, G., Liu, W., 2018. Sediment nitrogen cycling rates and microbial abundance along a submerged vegetation gradient in a eutrophic lake. Sci. Total Environ. 616-617, 899–907.

Yu, Z., Deng, H., Wang, D., Ye, M., Tan, Y., Li, Y., Chen, Z., Xu, S., 2013. Nitrous oxide emissions in the Shanghai river network: implications for the effects of urban sewage and IPCC methodology. Glob. Chang. Biol. 19, 2999–3010.

Zhang, F., Shi, X., Lian, S., Chen, Y., Lu, M., Feng, Q., Guo, R., 2022. A novel magnetic microparticles as biocarriers for promoting enrichment of nitrifying bacteria. J. Water Process Eng. 47, 102794.
Zhang, K., Qiu, Y., Zhao, Y., Wang, S., Deng, J., Chen, M., Xu, X., Wang, H., Bai, T., He, T., Zhang, Y., Chen, H., Wang, Y., Hu, S., 2023. Moderate precipitation reduction enhances nitrogen cycling and soil nitrous oxide emissions in a semi-arid grassland. Glob. Chang. Biol. 29, 3114–3129.
Zhou, Y., Suenaga, T., Qi, C., Riya, S., Hosomi, M., Terada, A., 2020. Temperature and oxygen level determine N_2O respiration activities of heterotrophic N_2O-reducing bacteria: biokinetic study. Biotechnol. Bioeng. 118, 1330–1341.